energies

MDPI

Article

Optimisation of Aggregate Demand Flexibility in Smart Grids and Wholesale Electricity Markets: A Bi-Level Aggregator Model Approach

Marco Toledo Orozco [1,*], Diego Morales [2], Yvon Bessanger [3], Carlos Álvarez Bel [1], Freddy H. Chuqui [4] and Javier B. Cabrera [5]

1 Institute for Energy Engineering, Universitat Politécnica de Valencia, Camino de Vera, 46022 Valencia, Spain
2 Circular Economy Laboratory-CIITT, Universidad Católica de Cuenca, Av. de las Américas, Cuenca 010107, Ecuador; dmoralesj@ucacue.edu.ec
3 Grenoble Electrical Engineering G2ELab, Université Grenoble Alpes, GreEn-ER, 21 Av. des Martyrs, 38000 Grenoble, France; yvon.besanger@g2elab.grenoble-inp.fr
4 Utility, Electro Generadora del Austro, Av. del Estadio, Cuenca 010215, Ecuador
5 Electrical Engineering, Universidad Católica de Cuenca, Av. de las Américas, Cuenca 010107, Ecuador; jcabreram@ucacue.edu.ec
* Correspondence: martoor@doctor.upv.es; Tel.: +593-984-364-210

Abstract

The transition toward intelligent and sustainable power systems requires practical schemes to integrate industrial demand flexibility into short-term operation, particularly in emerging electricity markets. This paper proposes an integrated framework that combines data-driven flexibility characterisation with a bi-level optimisation model for an industrial demand-side aggregator participating in the short-term balancing market. Flexibility is identified from AMI data and process information of large consumers, yielding around 2 MW of interruptible load and 3 MW of reducible load over a 24 h horizon. At the upper level, the aggregator maximises its profit by submitting flexibility offers; at the lower level, the system operator minimises balancing costs by co-optimising thermal generation and activated flexibility. The problem is formulated as a mixed-integer linear programming model and is evaluated on a real subtransmission and distribution network of a local utility in Ecuador, with ex-post power flow validation in DIgSILENT PowerFactory. Numerical results show that, despite the limited flexible capacity, the aggregator reduces the maximum energy price from USD/MWh 172.32 to 139.59 (about 19%), generating a daily revenue of USD 2475.15. From a network perspective, demand flexibility eliminates undervoltage at the most critical bus (from 0.93 to 1.03 p.u.) without creating overvoltages, while line loadings remain below 50% in all cases and total daily technical losses decrease from 89.46 to 89.10 MWh (about 0.4%). These results highlight both the potential and current limitations of industrial demand flexibility in short-term markets.

Keywords: demand flexibility; load disaggregation; NILMTK toolkit; aggregator model; bi-level optimization

Academic Editor: Michael Negnevitsky

Received: 17 November 2025
Revised: 12 December 2025
Accepted: 15 December 2025
Published: 27 December 2025

1. Introduction

The rapid transformation of modern distribution systems, driven by the growing penetration of DERs such as PV generation, energy storage systems, and flexible loads, has created operating conditions marked by increased variability, uncertainty, and technical constraints. Under these circumstances, traditional planning and operational strategies are insufficient to ensure voltage stability, reliability, and overall network efficiency. Recent analyses highlight demand-side flexibility as a key enabler to address these challenges, providing mechanisms for managing stochastic behaviour, alleviating congestion, reducing losses, and supporting voltage regulation across the distribution grid [1–3]. The digitalisation of distribution networks and the shift toward active grid architectures further emphasise the need for coordinated frameworks that integrate operators, prosumers, and local resources, where flexibility markets and transactive energy schemes generate economically efficient signals to orchestrate distributed assets [4]. Beyond routine operation, prosumer-based flexibility, particularly through PV and storage systems, enhances resilience by accelerating service restoration and improving reliability indices such as SAIDI and SAIFI [5]. Technical studies also demonstrate that maintaining operational feasibility under diverse conditions requires advanced methodologies for voltage regulation, dynamic control, and DER scheduling, all of which increasingly rely on flexible resources [6]. Parallel regulatory work highlights the importance of cost allocation mechanisms, risk management tools, and governance structures that support flexibility-oriented market designs [7,8]. Collectively, this body of work shows that DF is now indispensable for achieving reliable, efficient, and resilient distribution systems, motivating the need for its rigorous assessment and modelling to support modern operational architectures, local flexibility markets, and DER integration strategies capable of addressing the growing complexity of present day distribution networks [6,9,10].

1.1. Overview of Demand Flexibility in Smart Grids

Demand flexibility has become a central component in the development of smart grids, offering mechanisms to coordinate consumption, DERs, and market signals under increasing variability and uncertainty. The industrial sector has been widely recognised as one of the most promising domains for flexibility extraction. Early research demonstrated that industrial processes can modulate their electricity use without compromising product quality, laying the foundation for industrial DR. Building on these findings, Rodríguez-García et al. [11] employ a P-PSO algorithm to increase ancillary service participation by up to 40%, while Toledo-Orozco et al. [12] apply NILM and FHMM based disaggregation to estimate flexibility from limited metering data, enabling validated reductions of up to 50% in peak demand and 5% in annual consumption costs [13,14]. These results highlight the scalability of DF in industrial environments, even in systems with limited digitalisation or automation.

A second strand of research focuses on electricity markets and their evolving role in enabling DF participation. Market design strongly influences the economic potential of flexibility: Cabot and Villavicencio [15] show that regions with advanced DR and aggregation frameworks exhibited greater resilience during the 2021–2023 energy crisis, with lower price volatility and reduced balancing costs. Emerging digital architectures further expand these capabilities. Blockchain enabled flexibility markets [14] and decentralised P2P/ADMM market schemes [16] demonstrate improvements in price stability, fairness, and temporary grid independence. Forecasting also plays a crucial role: Rodríguez et al. [13] obtain MAPE values of 10.7–31.5% using RF models at 15-min resolution, while Nasab et al. [17] develop a MILP-based residential scheduling model that integrates dynamic pricing, PV, storage, and comfort preferences. Additionally, technological enablers such as AMI are essential for large-scale flexibility activation; Toledo-Orozco et al. [18] reveal that over 60% of existing meters require modernisation to support these advanced services.

Beyond market and technological dimensions, DF has far-reaching implications for system planning, distributed control, and renewable integration. Aggregators consolidate DERs, storage, EVs, and flexible loads into integrated portfolios capable of participating in electricity markets and responding to system needs in real time. Their effectiveness depends heavily on regulatory frameworks, revenue sharing models, and access to granular operational data, as highlighted by Okur et al. [19] and Hincapié [20]. At the system level, studies show that coordinated flexibility can reduce peak demand and defer network reinforcements: Backe et al. [21] report national peak reductions of 10–12% in highly electrified scenarios, while Askeland et al. [22] show that community based flexibility reduces grid capacity needs by 13.1% and total system costs by 1.8%. EVs also represent an increasingly influential source of flexibility; Syla et al. [23] demonstrate that smart charging and V2G strategies can reduce system costs by up to 29% and stationary storage requirements by 19–37%, while LP-based EV charging models further highlight the need to integrate mobility patterns and network constraints. Finally, market-based flexibility procurement mechanisms such as pay-as-bid auctions [24] show potential for increasing social welfare under high DER penetration, although the lack of standardisation in flexibility quantification remains a major barrier [25]. Altogether, the literature confirms that DF is a technically feasible and economically valuable resource for modern power systems. The works synthesised in Table 1 provide the methodological foundations adopted in this study. These references encompass NILM-based disaggregation, industrial flexibility characterisation, IEC-based interoperability, economic valuation, and aggregator operational models. Collectively, they support the development of the integrated framework proposed in this work for quantifying and optimising the flexibility managed by the aggregator.

Table 1. Demand aggregation and flexibility: a summary of the state of the art in operations research.

Section	Main topic	Subtopic	References
Introduction	–	–	[1–3,6,9]
Methodology for acquisition, structuring, and analysis of information	NILMTK toolkit for load monitoring	–	[12,26]
	Information acquisition	Data structuring	[18]
	Supervised/semi-supervised learning	Learning paradigms	[27]
Load profile disaggregation and flexibility assessment	ML algorithms for disaggregation	Combinatorial optimisation	[28]
	FHMM/HMM models	NILM-based modelling	[12,29]
Aggregator model and market participation	Aggregator business models in DSOs	DR strategies/coordination mechanisms	[15,19,30]

1.2. Contributions

Although DF has demonstrated technical, economic, and environmental benefits, several challenges still hinder its large-scale implementation. Industrial consumers continue to exploit only a fraction of their flexible potential, and many existing approaches remain focused on isolated sectors or specific market products. Furthermore, current methodologies do not fully integrate flexibility characterisation, market participation, and coordinated operation among DSOs, TSOs, and aggregators, particularly in environments with limited metering infrastructure or emerging electricity markets. These limitations highlight the need for comprehensive frameworks that connect flexibility identification with its practical activation at both operational and market levels.

To address these challenges, this work makes four main contributions:

- A data-driven methodology for identifying and quantifying industrial flexibility using AMI data, NILM techniques, and process-level information, generating flexibility blocks that incorporate technical, economic, and production constraints.
- An interoperability-based information architecture for smart distribution systems, built on IEC standards, enabling coordinated activation of flexibility through seamless integration among metering systems, data management platforms, DER management, and the aggregator.
- A bi-level optimisation model for an aggregator participating in short-term balancing markets, where the upper level maximises profit through flexible demand and the lower level minimises system balancing costs under network and operational constraints, formulated as an MILP problem.
- A validation on a real distribution system that demonstrates the impact of aggregated flexibility on network operation, using hourly demand profiles and energy costs from the Ecuadorian power system. The assessment is carried out through power flow studies in DIgSILENT PowerFactory, enabling the quantification of its effects on voltages, loading levels, and losses in the distribution network.

The remainder of this paper is structured as follows: Section 2 presents the methodology for identifying and quantifying demand flexibility in large consumer systems using NILMTK, AMI measurements, and data analytics. Section 3 examines the operational implications of flexibility in smart distribution systems, with emphasis on interoperability and information integration. Section 4 introduces the proposed bi-level optimisation model for demand aggregation and flexibility participation in the short-term market. Section 5 details the real-world case study, based on a subtransmission and distribution network of a local utility in Ecuador, including 28 large consumers and actual hourly demand and energy cost data. Section 6 presents and discusses the numerical results, quantifying the impact of aggregated industrial flexibility on short-term balancing costs, bus voltage profiles, line and transformer loading. Finally, Section 7 summarises the main conclusions and outlines future research directions.

2. Methodology for Determining and Quantifying Demand Flexibility

2.1. Integration and Data Acquisition for Modelling Demand Disaggregation

For the disaggregation of demand in LC, the information was obtained directly from the commercial meter installed by the distribution system operator, following the approach applied in [12]. Based on the total load profile recorded at the delivery point, the data were cleaned, validated, and organised into a uniform structure suitable for further processing. This preprocessing involved correcting missing or inconsistent values and generating a continuous time series with the required resolution for analysis.

Once structured, the records were converted into the format required by the NILMTK toolkit, enabling the application of non-intrusive load disaggregation algorithms to reconstruct the consumption associated with each industrial process without the need for circuit-level measurements. This integration workflow, which starts from raw AMI measurements and culminates in disaggregated load profiles, forms the basis for identifying interruptible and reducible demand flexibility blocks. Figure 1 provides an overview of the main stages considered in this procedure.

https://doi.org/10.3390/en19010152

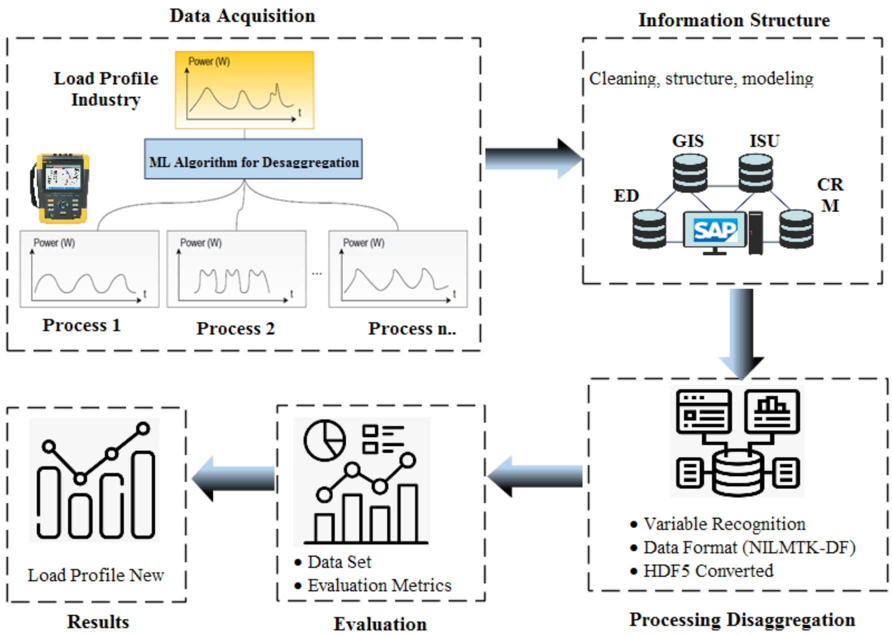

Figure 1. The methodological workflow for the acquisition, structuring, and disaggregation of industrial demand data, adapted from [12].

2.2. Nilmtk Toolkit for the Disaggregation of Load Profiles in LC

To disaggregate the demand of the LC, the NILMTK toolkit was used following the procedure described in [12]. Based on the preprocessed AMI profile, the data were transformed into the NILMTK-DF structure, and the disaggregation algorithms included in the toolkit, mainly FHMM, were applied to separate the total consumption into the main industrial processes without requiring additional circuit-level metering. The performance of the disaggregation was evaluated using the EAE, MNEAP, RMSE, and F1 metrics, ensuring consistency between the estimated profiles and the expected behaviour of each process.

2.3. Analysis of Production Variables to Determine the Flexibility of LC

The aggregated demand measured at the delivery point was first disaggregated using NILMTK models trained according to [12]. These models, configured with validated training ratios and sampling intervals (2–30 min) based on the ECDIAC dataset, enabled the reconstruction of the individual consumption of each industrial process from the AMI profile. With the disaggregated profiles, the technical, economic, and production variables were analysed using the DRIP tool [28]. This evaluates key parameters, including nominal power, operational cycles, minimum on/off times, interruption-related costs, production sensitivity to load variations, and process continuity constraints. Based on these variables, DRIP classifies processes according to their end-use category and their ability to undergo interruption or controlled reduction. This classification enables the identification of available power, feasible time windows, and the type of flexibility (interruptible or reducible), forming the flexibility blocks that serve as input for the operational and economic evaluation performed by the aggregator.

3. Interoperability of Flexibility and Stakeholder Participation in the Operation of Distribution Systems

The effective activation of flexibility in modern distribution systems requires an interoperable architecture that can coordinate all actors and platforms involved in both local and system-level operations. As illustrated in Figure 2, the proposed framework is intentionally generic: flexibility circulates through a structured network of energy flows, contractual relationships, and information exchanges that link the Active Client, the Aggregator, the DSO, the BRP, and the TSO, together with DER such as PV, BESS, and EV. These resources are shown in the figure as examples of assets that can be integrated within the same architecture; however, in the case study analysed in this work, the flexibility modelled in the optimisation problem arises exclusively from large industrial consumers and BESS units. PV plants are represented as local distributed generation whose main role is to supply demand and charge the batteries, thereby reducing energy purchases from the grid, while EVs are not explicitly included in the optimisation model.

This framework reflects the coexistence of implicit flexibility, derived from demand disaggregation and forecasting at the client level, and explicit flexibility, transacted through formal arrangements such as balancing services, congestion management, or curtailment services. Within this ecosystem, the Aggregator acts as the central node, consolidating, validating, and commercialising flexibility and performing the roles of BSP, CMSP, or CSP according to the service requested by the FRP. Reliable interaction among these agents requires an information architecture based on IEC 61968 [31] , which defines standardised semantic models and interfaces that enable bidirectional communication among AMI systems, MDM platforms, DER management modules, and DMS/ADMS environments. This IEC-based interoperability layer reduces technological barriers, ensures consistent data exchange, and enables coordinated and verifiable activation of flexibility across heterogeneous resources, forming a key component for smart distribution system operation and for the deployment of local flexibility markets.

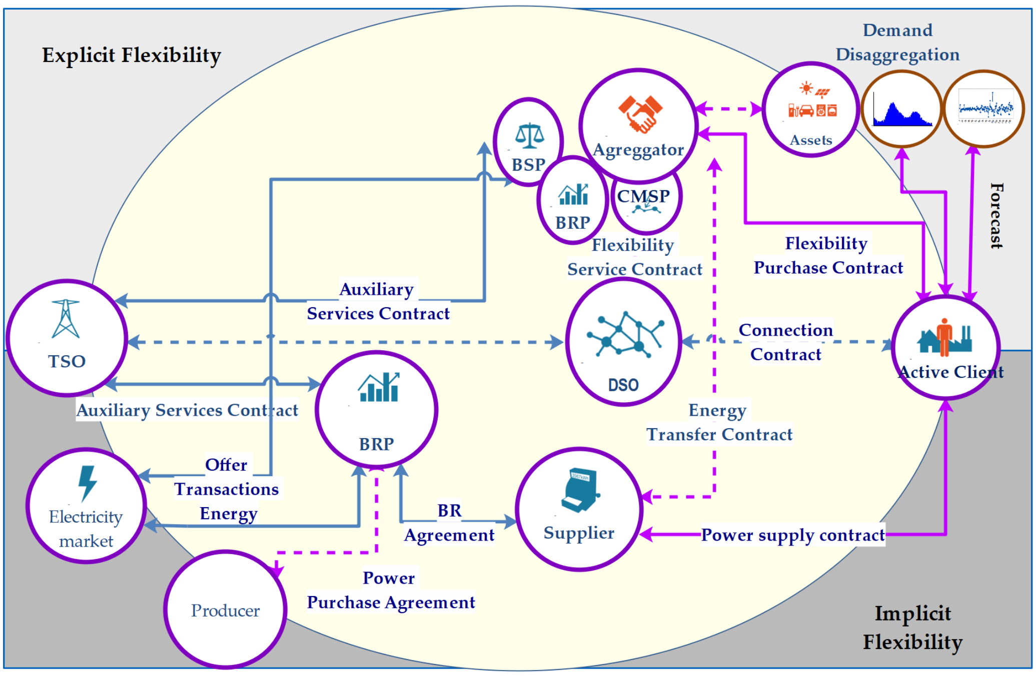

Figure 2. Stakeholder participation in the new architecture of demand flexibility and DERs.

4. Aggregator Model and Bi-Level Optimisation

In this work, the aggregator is modelled as an intermediary entity that coordinates the operation of the DF provided by a portfolio of LC. Its objective is to exploit the available flexibility in an optimal way in order to maximise the economic benefit of the aggregator's portfolio, while at the same time contributing to the technical and economic balance of the power system.

The aggregator operates in the short-term market, compensating for the differences between planned and actual values. The aggregator does not participate in the day-ahead markets, as the volume of energy it manages represents a small fraction of the total system demand, and therefore its individual buy or sell decisions do not significantly impact market prices.

DA prices are treated as exogenous signals in the model, and the optimisation problem of the aggregator consists of determining, for each hourly period, the optimal quantities of demand to be flexibilized, with the objective of maximising its profit.

In the short-term market, the aggregator participates actively by adjusting its flexible demand in response to deviations between planned and actual values. In this context, the activation of aggregated flexibility can influence balancing prices, as it contributes to decreasing or increasing the net imbalance that must be corrected by the TSO/DSO, and therefore affects the overall balancing costs of the system.

4.1. Mathematical Model

In the proposed formulation, the network physics are not represented explicitly within the mathematical model. Instead, once the optimisation results are obtained, they are validated through power flow studies carried out using DIgSILENT PowerFactory 2025. In this way, the model focuses on operational decision-making and on the economic valuation of flexibility, while the verification of electrical feasibility is performed ex post through network analysis.

Consequently, the optimisation results must be interpreted as market-level scheduling decisions and economic outcomes for the aggregator, subject to subsequent verification of their technical feasibility through network power flow calculations.

4.2. Upper Level Problem

The main objective is to maximise the profits obtained by the aggregator through participation in the short-term market by submitting strategic offers based on the proper dispatch of demand response contracts.

$$\max \sum_{t \in T} \left[\gamma_t \cdot \left(P_t^{A,\mathcal{B}_U} - P_t^{A,\mathcal{B}_L} \right) \cdot \Delta t \right] \tag{1}$$

Subject to:

$$P_{t,i}^{I} = \overline{P_{t,i}^{I}}\, \alpha_{t,i}^{I} \quad \forall t \in T, \forall i \in GC \tag{2}$$

$$0 \leq P_{t,i}^{\mathcal{R}} \leq \overline{P_{t,i}^{\mathcal{R}}} \quad \forall t \in T, \forall i \in GC \tag{3}$$

$$P_t^{A,\mathcal{B}_U} = \sum_{i \in GC} \left(P_{t,i}^{I} + P_{t,i}^{\mathcal{R}} \right) \quad \forall t \in T \tag{4}$$

Equation (1) models the economic benefit of the aggregator when participating in the short-term market by selling flexible energy at an hourly price γ_t. Equation (2) enforces that interruptible energy can only be activated in full blocks, consistent with the volume originally offered by each LC. Equation (3) constrains the reducible energy of each LC not to exceed its maximum reduction capability. Finally, Equation (4) defines the total energy that the aggregator can offer at time t as the sum of the interruptible and reducible energies enabled from all participating LC.

4.3. Lower Level Problem

The objective is to minimise the costs associated with system balancing through the provision of balancing services in the short-term market. The decision variables include the power supplied by both the participating generators and the aggregator to adjust supply and demand. It is essential to note that the aggregator's offer is considered fixed at this level, as it was previously determined in the upper-level problem.

$$\min \sum_{t \in T} \left[\sum_{i \in G} \left(C^U_{t,i} P^U_{t,i} - C^L_{t,i} P^L_{t,i} \right) + \beta_t \left(P_t^{A,\mathcal{B}_U} - P_t^{A,\mathcal{B}_L} \right) \right] \cdot \Delta t \tag{5}$$

Subject to:

$$P_t^S + \sum_{i \in G} (P^U_{t,i} - P^L_{t,i}) + P_t^{A,\mathcal{B}_U} - P_t^{A,\mathcal{B}_L} = P_t^B \tag{6}$$

$$0 \le P^U_{t,i} \le \overline{P^U_{t,i}} \quad \forall t \in T, \forall i \in G \tag{7}$$

$$0 \le P^L_{t,i} \le \overline{P^L_{t,i}} \quad \forall t \in T, \forall i \in G \tag{8}$$

$$0 \le P_t^{A,\mathcal{B}_U} \le \overline{P_t^{A,\mathcal{B}_U}} \quad \forall t \in T \tag{9}$$

$$0 \le P_t^{A,\mathcal{B}_L} \le \overline{P_t^{A,\mathcal{B}_L}} \quad \forall t \in T \tag{10}$$

Equation (5) defines the objective function of the lower level problem, which minimizes the total cost of the balancing service in the short-term electricity market. The first term sums the marginal costs of upward and downward regulation of the participating generators, whereas the second term represents the cost associated with activating the upward and downward flexibility of the aggregator, computed at the balancing price β_t, which is treated as an exogenous parameter fixed by the upper-level problem. Equation (6) enforces the real time power balance in the balancing market. For each time interval t, the day-ahead scheduled generation, together with the net regulation of the participating generators and the net balancing power provided by the aggregator, must equal the real time balancing demand P_t^B. Finally, constraints (7) and (8) define the operating limits for the upward and downward regulation of each generator, enforcing that $P^U_{t,i}$ and $P^L_{t,i}$ are non negative and do not exceed their respective maximum capacities $\overline{P^U_{t,i}}$ and $\overline{P^L_{t,i}}$, as determined by the technical limits and the day ahead schedule of each unit. Similarly, Constraints (9) and (10) bound the upward and downward balancing power of the aggregator, requiring $P_t^{A,\mathcal{B}_U}$ and $P_t^{A,\mathcal{B}_L}$ to lie between zero and their maximum values $\overline{P_t^{A,\mathcal{B}_U}}$ and $\overline{P_t^{A,\mathcal{B}_L}}$, which represent the aggregated flexibility available from the portfolio of LC at each time interval.

It is important to note that, in the case study considered, the aggregator can only provide upward balancing, since it does not hold differentiated duration contracts that would allow it to shift its customers' consumption to other time intervals. Nevertheless, the model has been formulated in a general way, also including downward balancing, so that in future scenarios where the aggregator has access to this type of contract, the extension and implementation of the scheme become straightforward.

4.4. Transformation into a Single Level Mixed Integer Linear Programming Problem (MILP)

Based on the linear formulation of the lower-level problem and following classical optimality criteria, the Karush–Kuhn–Tucker (KKT) conditions are both necessary and sufficient to ensure the optimality of the said problem [32–34]. In this context, it is possible to incorporate these conditions into the upper-level problem, thereby transforming it into a single-level optimisation problem. Both levels are merged into a unified optimisation formulation by embedding the KKT conditions into the upper-level problem. This approach simplifies the solution optimisation by deriving an optimal solution that satisfies both the upper-level constraints and the optimality conditions of the lower level. In this way, the strategy of combining both problems into a single formulation facilitates the search for a global solution that maximises the profit of the aggregator in the electricity market, while simultaneously ensuring compliance with the technical and economic constraints of the system.

Kkt Conditions

- Primal feasibility: Constraints (6)–(10)
- Stationarity

$$\mathbb{C}^U_{t,i} + \lambda^1_{t,i} - \lambda^2_{t,i} - \gamma_t = 0 \qquad \forall t \in T,\ \forall i \in G \tag{11}$$

$$-\mathbb{C}^L_{t,i} + \lambda^3_{t,i} - \lambda^4_{t,i} + \gamma_t = 0 \qquad \forall t \in T,\ \forall i \in G \tag{12}$$

$$\beta_t + \lambda^5_t - \lambda^6_t - \gamma_t = 0 \qquad \forall t \in T \tag{13}$$

$$-\beta_t + \lambda^7_t - \lambda^8_t + \gamma_t = 0 \qquad \forall t \in T \tag{14}$$

In this system, the dual variables $\lambda^1_{t,i}$, $\lambda^2_{t,i}$, $\lambda^3_{t,i}$, $\lambda^4_{t,i}$, λ^5_t, λ^6_t, λ^7_t, and λ^8_t are the Lagrange multipliers associated with the bound and flexibility constraints of the primal problem, and therefore capture the marginal value of relaxing each of these constraints in the short-term market.

- Dual feasibility and complementary slackness

The following conditions impose dual feasibility and complementary slackness for the lower-level problem, using the complementarity notation $0 \leq x \perp y \geq 0$, which implies $x \geq 0$, $y \geq 0$, and $x \cdot y = 0$. In particular, each dual variable $\lambda^1_{t,i}, \ldots, \lambda^4_{t,i}, \lambda^5_t, \ldots, \lambda^8_t$ is associated with the upper or lower bound of the corresponding flexible power and block-offer variables. Under this notation, a dual variable can be strictly positive only when its associated bound is binding; otherwise, the multiplier is zero and the primal variable remains strictly inside its admissible interval.

$$x \geq 0, \quad y \geq 0, \quad \text{and} \quad x \cdot y = 0.$$

$$0 \leq \lambda^1_{t,i} \perp \left(\overline{P^U_{t,i}} - P^U_{t,i}\right) \geq 0 \quad \forall t \in T,\ \forall i \in G \tag{15}$$

$$0 \leq \lambda^2_{t,i} \perp P^U_{t,i} \geq 0 \quad \forall t \in T,\ \forall i \in G \tag{16}$$

$$0 \leq \lambda^3_{t,i} \perp \left(\overline{P^L_{t,i}} - P^L_{t,i}\right) \geq 0 \quad \forall t \in T,\ \forall i \in G \tag{17}$$

$$0 \leq \lambda^4_{t,i} \perp P^L_{t,i} \geq 0 \quad \forall t \in T,\ \forall i \in G \tag{18}$$

$$0 \leq \lambda^5_t \perp \left(\overline{P^{A,\mathcal{B}_U}_t} - P^{A,\mathcal{B}_U}_t\right) \geq 0 \quad \forall t \in T \tag{19}$$

$$0 \leq \lambda^6_t \perp P^{A,\mathcal{B}_U}_t \geq 0 \quad \forall t \in T \tag{20}$$

$$0 \leq \lambda^7_t \perp \left(\overline{P^{A,\mathcal{B}_L}_t} - P^{A,\mathcal{B}_L}_t\right) \geq 0 \quad \forall t \in T \tag{21}$$

$$0 \leq \lambda^8_t \perp P^{A,\mathcal{B}_L}_t \geq 0 \quad \forall t \in T \tag{22}$$

Since constraints (15)–(22) are not linear, the Fortuny-Amat transformation [35] is used. This approach converts these equations into two linear constraints by applying the "Big M" technique along with binary variables. The expression used for this transformation is as follows:

$$0 \leq x \leq M \cdot u, \quad 0 \leq y \leq M \cdot (1-u), \quad u \in \{0,1\}$$

In this sense, constraints (15)–(22) can be linearised, since they satisfy all the conditions mentioned above. The new set of constraints that replaces the original ones is as follows:

$$0 \leq \lambda^1_{t,i} \leq M \cdot u^{\lambda_1} \quad \forall t \in T,\ \forall i \in G \tag{23}$$

$$\overline{P^U_{t,i}} - P^U_{t,i} \leq M \cdot (1 - u^{\lambda_1}) \quad \forall t \in T, \forall i \in G \tag{24}$$

$$0 \leq \lambda^2_{t,i} \leq M \cdot u^{\lambda_2} \quad \forall t \in T, \forall i \in G \tag{25}$$

$$P^U_{t,i} \leq M \cdot (1 - u^{\lambda_2}) \quad \forall t \in T, \forall i \in G \tag{26}$$

$$0 \leq \lambda^3_{t,i} \leq M \cdot u^{\lambda_3} \quad \forall t \in T, \forall i \in G \tag{27}$$

$$\overline{P^L_{t,i}} - P^L_{t,i} \leq M \cdot (1 - u^{\lambda_3}) \quad \forall t \in T, \forall i \in G \tag{28}$$

$$0 \leq \lambda^4_{t,i} \leq M \cdot u^{\lambda_4} \quad \forall t \in T, \forall i \in G \tag{29}$$

$$P^L_{t,i} \leq M \cdot (1 - u^{\lambda_4}) \quad \forall t \in T, \forall i \in G \tag{30}$$

$$0 \leq \lambda^5_{t,i} \leq M \cdot u^{\lambda_5} \quad \forall t \in T \tag{31}$$

$$\overline{P^{A,\mathcal{B}_U}_t} - P^{A,\mathcal{B}_U}_t \leq M \cdot (1 - u^{\lambda_5}) \quad \forall t \in T \tag{32}$$

$$0 \leq \lambda^6_{t,i} \leq M \cdot u^{\lambda_6} \quad \forall t \in T \tag{33}$$

$$P^{A,\mathcal{B}_U}_t \leq M \cdot (1 - u^{\lambda_6}) \quad \forall t \in T \tag{34}$$

$$0 \leq \lambda^7_{t,i} \leq M \cdot u^{\lambda_7} \quad \forall t \in T \tag{35}$$

$$\overline{P^{A,\mathcal{B}_L}_t} - P^{A,\mathcal{B}_L}_t \leq M \cdot (1 - u^{\lambda_7}) \quad \forall t \in T \tag{36}$$

$$0 \leq \lambda^8_{t,i} \leq M \cdot u^{\lambda_8} \quad \forall t \in T \tag{37}$$

$$P^{A,\mathcal{B}_L}_t \leq M \cdot (1 - u^{\lambda_8}) \quad \forall t \in T \tag{38}$$

By incorporating all the Kkt conditions into the upper-level problem, the model remains nonlinear due to the term $\gamma_t \cdot \left(P^{A,\mathcal{B}_U}_t - P^{A,\mathcal{B}_L}_t\right)$ present in the objective function at this level. To linearise this term, the strong duality theorem is applied. Since the lower-level problem is linear, strong duality holds, which implies that the optimal values of the primal and dual problems are equal.

According to the duality theorem, at the optimum, the following condition holds:

$$\begin{aligned} &\sum_{t \in T} \sum_{i \in G} \left(\mathbb{C}^U_{t,i} \cdot P^U_{t,i} - \mathbb{C}^L_{t,i} \cdot P^L_{t,i}\right) \\ &\qquad + \sum_{t \in T} \beta_t \cdot \left(P^{A,\mathcal{B}_U}_t - P^{A,\mathcal{B}_L}_t\right) \\ &= \sum_{t \in T} \Bigg[- \gamma_t \cdot \left(P^B_t - P^S_t\right) - \sum_{i \in G} \Big(\lambda^1_{t,i} \cdot \overline{P^U_{t,i}} + \lambda^3_{t,i} \cdot \overline{P^L_{t,i}} \\ &\qquad + \lambda^5_{t,i} \cdot \overline{P^{A,\mathcal{B}_U}_t} + \lambda^7_{t,i} \cdot \overline{P^{A,\mathcal{B}_L}_t}\Big)\Bigg] \end{aligned} \tag{39}$$

By rearranging the terms in Equations (13) and (14); multiplying them by $P^{A,\mathcal{B}_U}_t$ and $P^{A,\mathcal{B}_L}_t$, respectively; and summing over t, the following expression is obtained:

$$\sum_{t \in T} \beta_t \cdot P^{A,\mathcal{B}_U}_t = \sum_{t \in T} \left(-\lambda^5_t + \lambda^6_t + \gamma_t\right) \cdot P^{A,\mathcal{B}_U}_t \tag{40}$$

$$\sum_{t \in T} \beta_t \cdot P^{A,\mathcal{B}_L}_t = \sum_{t \in T} \left(\lambda^7_t - \lambda^8_t + \gamma_t\right) \cdot P^{A,\mathcal{B}_L}_t \tag{41}$$

By rearranging Equations (19) and (21) and summing over t, the following expression is obtained:

$$\sum_{t\in T} \lambda^5_{t,i} \cdot \overline{P^{A,\mathcal{B}_U}_t} = \sum_{t\in T} \lambda^5_{t,i} \cdot P^{A,\mathcal{B}_U}_t \tag{42}$$

$$\sum_{t\in T} \lambda^7_{t,i} \cdot \overline{P^{A,\mathcal{B}_L}_t} = \sum_{t\in T} \lambda^7_{t,i} \cdot P^{A,\mathcal{B}_L}_t \tag{43}$$

By substituting Equations (42) and (43) into (40) and (41), respectively, the following is obtained:

$$\sum_{t\in T} \beta_t \cdot P^{A,\mathcal{B}_U}_t = \sum_{t\in T} \Big(-\lambda^5_{t,i} \cdot \overline{P^{A,\mathcal{B}_U}_t} + \lambda^6_t \cdot P^{A,\mathcal{B}_U}_t + \gamma_t \cdot P^{A,\mathcal{B}_U}_t \Big) \tag{44}$$

$$\sum_{t\in T} \beta_t \cdot P^{A,\mathcal{B}_L}_t = \sum_{t\in T} \Big(\lambda^7_{t,i} \cdot \overline{P^{A,\mathcal{B}_L}_t} - \lambda^8_t \cdot P^{A,\mathcal{B}_L}_t + \gamma_t \cdot P^{A,\mathcal{B}_L}_t \Big) \tag{45}$$

By substituting these terms into Equation (39), the following expression is obtained:

$$\begin{aligned}
&\sum_{t\in T}\sum_{i\in G}\Big(\mathbb{C}^U_{t,i} \cdot P^U_{t,i} - \mathbb{C}^L_{t,i} \cdot P^L_{t,i}\Big) + \sum_{t\in T}\Big(-\lambda^5_{t,i} \cdot \overline{P^{A,\mathcal{B}_U}_t} \\
&\quad + \lambda^6_t \cdot P^{A,\mathcal{B}_U}_t + \gamma_t \cdot P^{A,\mathcal{B}_U}_t - \lambda^7_{t,i} \cdot \overline{P^{A,\mathcal{B}_L}_t} \\
&\quad + \lambda^8_t \cdot P^{A,\mathcal{B}_L}_t - \gamma_t \cdot P^{A,\mathcal{B}_L}_t \Big) \\
&= \sum_{t\in T}\Big[-\gamma_t \cdot \Big(P^B_t - P^S_t\Big) - \lambda^5_{t,i} \cdot \overline{P^{A,\mathcal{B}_U}_t} - \lambda^7_{t,i} \cdot \overline{P^{A,\mathcal{B}_L}_t} \\
&\quad - \sum_{i\in G}\Big(\lambda^1_{t,i} \cdot \overline{P^U_{t,i}} + \lambda^3_{t,i} \cdot \overline{P^L_{t,i}}\Big)\Big]
\end{aligned} \tag{46}$$

Note that the terms $\lambda^7_{t,i} \cdot \overline{P^{A,\mathcal{B}_L}_t}$ and $\lambda^5_{t,i} \cdot \overline{P^{A,\mathcal{B}_U}_t}$ cancel out, according to Equation (20), and the terms $\lambda^6_t \cdot P^{A,\mathcal{B}_U}_t$ and $\lambda^8_t \cdot P^{A,\mathcal{B}_L}_t$ are equal to zero. In this way, it is possible to compute the nonlinear term of the upper-level problem.

$$\begin{aligned}
\sum_{t\in T} \gamma_t \cdot \Big(P^{A,\mathcal{B}_U}_t - P^{A,\mathcal{B}_L}_t\Big) &= -\sum_{t\in T} \gamma_t \cdot \Big(P^B_t - P^S_t\Big) \\
&\quad - \sum_{i\in G}\Big[\Big(\mathbb{C}^U_{t,i} \cdot P^U_{t,i} - \mathbb{C}^L_{t,i} \cdot P^L_{t,i}\Big) + \lambda^1_{t,i} \cdot \overline{P^U_{t,i}} + \lambda^3_{t,i} \cdot \overline{P^L_{t,i}}\Big]
\end{aligned} \tag{47}$$

Final Model

$$\begin{aligned}
\max \sum_{t\in T}\Big[&-\gamma_t \cdot \Big(P^B_t - P^S_t\Big) \\
&- \sum_{i\in G}\Big(\Big(\mathbb{C}^U_{t,i} \cdot P^U_{t,i} - \mathbb{C}^L_{t,i} \cdot P^L_{t,i}\Big) + \Big(\lambda^1_{t,i} \cdot \overline{P^U_{t,i}} + \lambda^3_{t,i} \cdot \overline{P^L_{t,i}}\Big)\Big)\Big]
\end{aligned} \tag{48}$$

Subject to:

- Upper-level constraints (2)–(4)
- Primal feasibility (6)–(10)
- Stationarity (11)–(14)
- Dual feasibility and complementary slackness (23)–(38)

The bi-level model was implemented in Python 3.12 using the Pyomo library and solved with the GLPK solver.

5. Case Study

To validate the proposed model, hourly demand and energy cost data from the Ecuadorian power system are used. In this context, generators participate in the market by offering their production at the marginal costs declared for each plant, whereas the aggregator provides flexibility services by adjusting its energy sales offers in response to the price signal.

The aggregator's portfolio consists of 28 LC, for which hourly reducible and interruptible power is available. The impact of activating this flexibility is assessed through power flow studies on the distribution network of Empresa Eléctrica Regional Centro Sur, comparing a reference scenario without flexibility against a scenario with flexibility activation. This analysis examines bus voltage profiles, line and transformer loading, and technical losses.

The methodology for defining short-term energy selling prices is based on the hourly marginal cost, understood as the cost of the last generating unit that provides the system balance. Figure 3 shows the energy selling costs together with the system demand for each hourly interval. Figure 4 presents the aggregated reducible and interruptible power of all large consumers, also disaggregated by hourly interval.

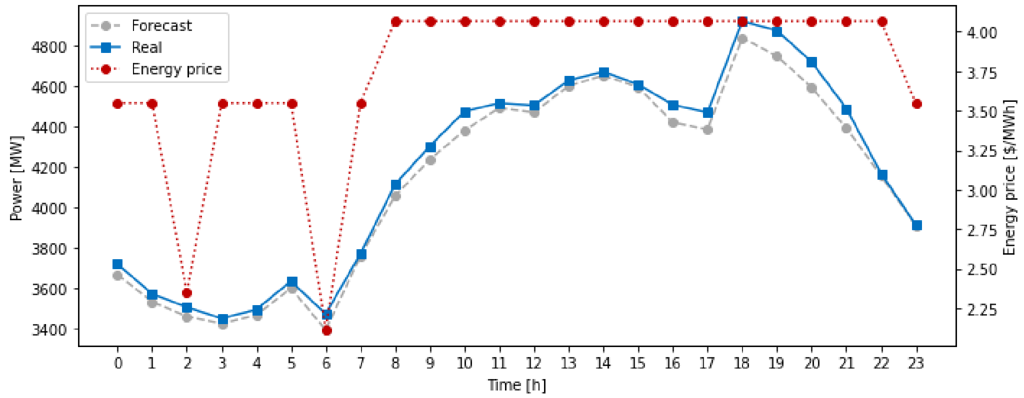

Figure 3. Scheduled and real system demand and energy price.

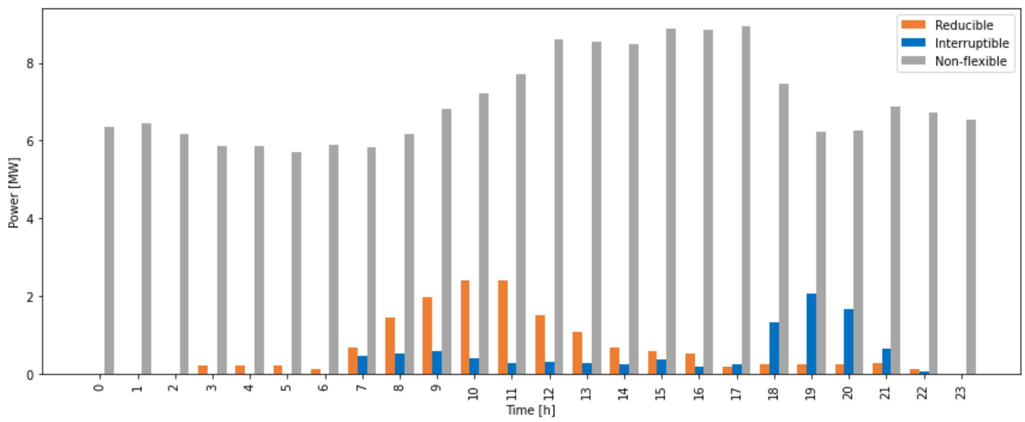

Figure 4. Aggregated reducible and interruptible demand flexibility of LC.

6. Analysis of Results

6.1. Demand Flexibility

The flexibility assessment revealed that the 28 large consumers analysed provide a significant contribution to system operability through both interruptible and reducible demand. As shown in Figure 5, the disaggregation and classification of industrial processes allowed the identification of approximately 2 MW of interruptible load and 3 MW of reducible load within a 24 h window. The interruptible segments exhibit typical activation durations of 2–4 h, whereas reducible segments range from 2–5 h, corresponding to 25–45% of each consumer's maximum demand. These flexibility blocks capture both the magnitude and temporal availability of modulation capabilities across various sectors, including ceramics, plastics, food processing, and commercial facilities. Figure 6 illustrates representative flexibility profiles for four distinct consumers, evidencing different operational behaviours and energy-use patterns.

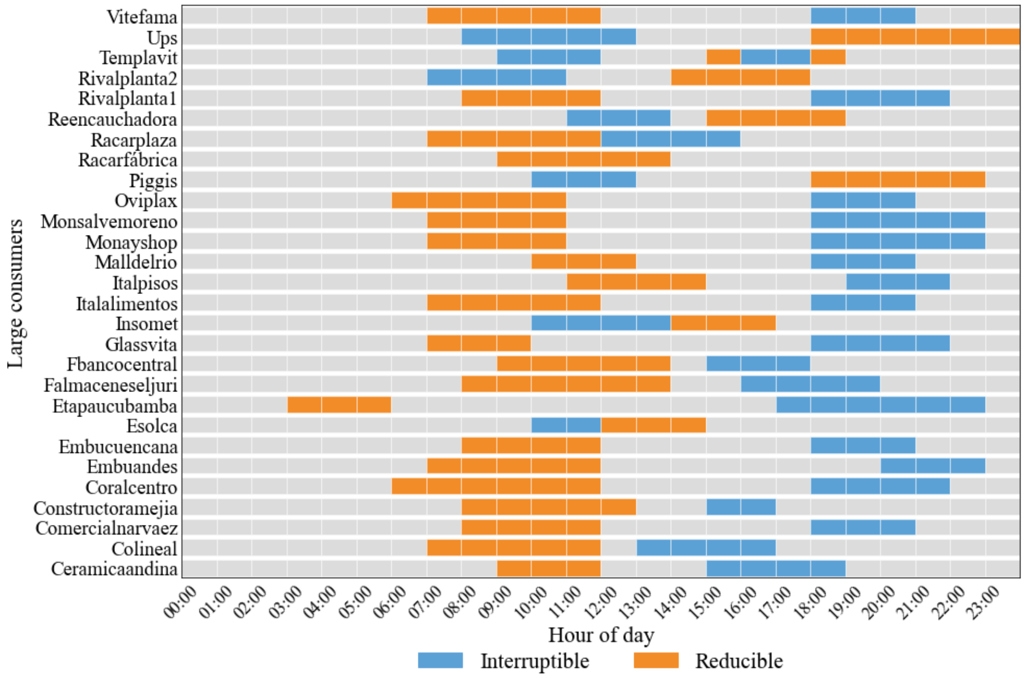

Figure 5. Interruptible and reducible energy blocks from the DF assessment.

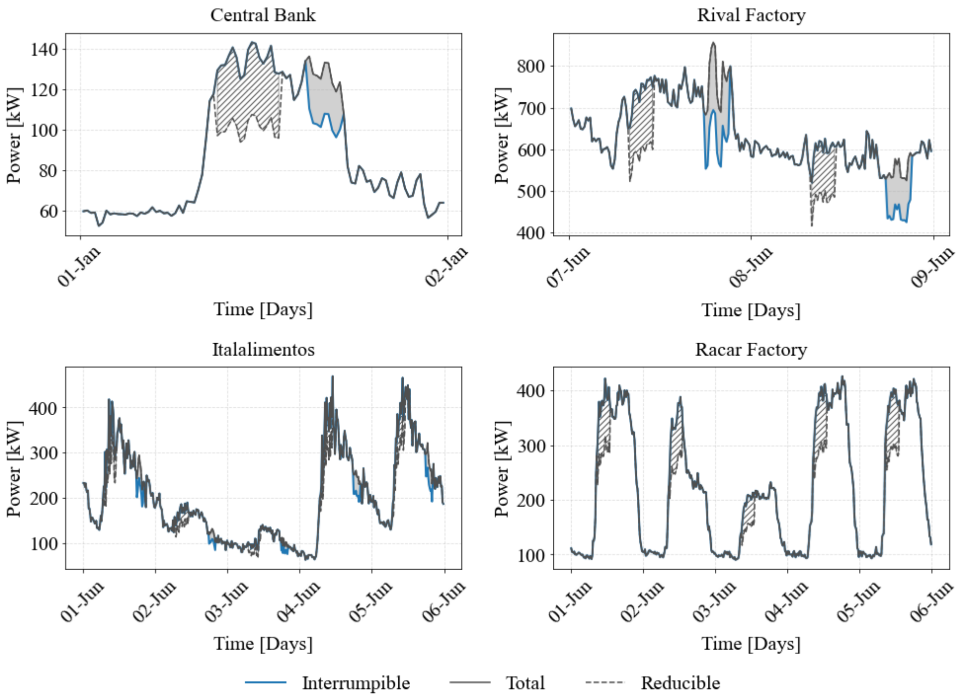

Figure 6. Examples of DF in LC, representative DF daily profiles.

6.2. Scenario 1—No Flexibility Demand

In the base scenario, without activating demand flexibility, system balancing in the short-term market is carried out exclusively through the generation of participating thermal units. As shown in Figures 7 and 8, for most hours of the day, the hourly energy price remains close to the minimum value of USD/MWh 91.27, primarily supplied by lower-cost units during periods of low and medium demand. However, between 19:00 and 20:00, the highest balancing energy requirement occurs, on the order of 127 MWh, which forces the system to dispatch a high-cost unit. At those hours, generator 22 becomes the marginal unit, contributing only 1.71 MWh and 1.34 MWh, respectively, but enough to cover the last segment of demand and set the market price at USD/MWh 172.32. This highlights the impact of merit-order dispatch: small contributions from expensive units at the margin can produce significant price spikes, increasing the cost of the entire volume of energy traded in those periods.

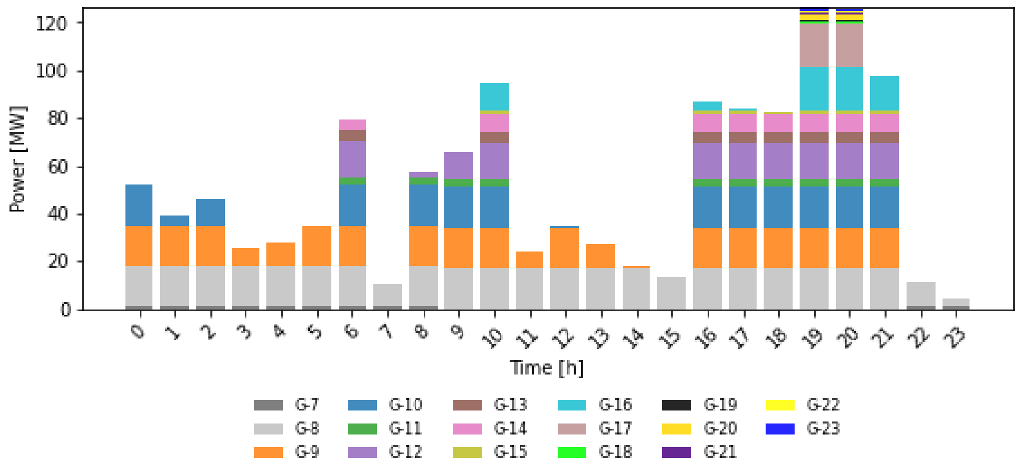

Figure 7. Hourly dispatch of thermal generators in the scenario without demand flexibility.

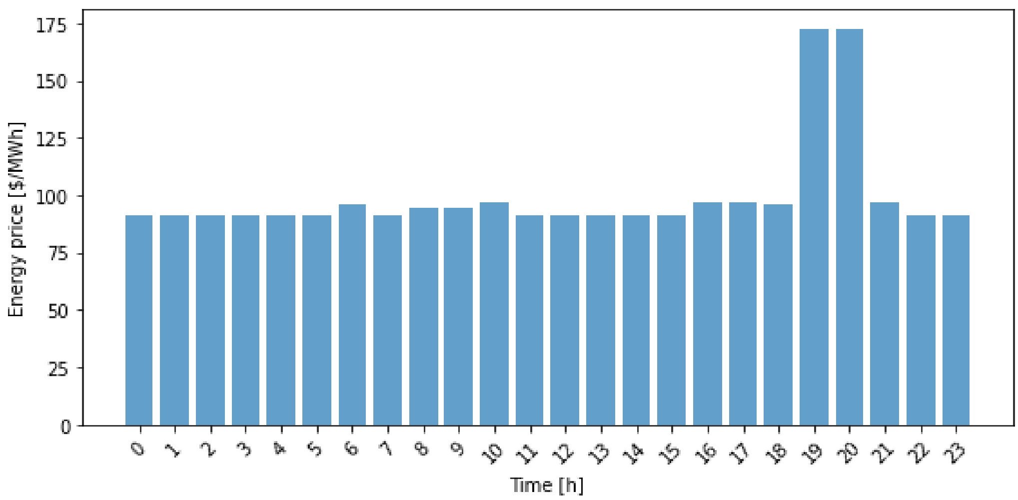

Figure 8. Energy prices in the scenario without demand flexibility.

6.3. Scenario 2—Flexibility Demand

In this scenario, system imbalances in the short-term market are covered in a coordinated manner by thermal generation and by the activation of demand flexibility managed by the aggregator. Unlike the base case, where the maximum energy price reaches USD/MWh 172.32, in this scenario it is reduced to USD/MWh 139.59, as shown in Figures 9 and 10, which corresponds to the marginal cost of thermal generator 21. During peak hours, this unit operates at its maximum output and the residual power required to close the balance is provided by the aggregator through flexible demand reduction. This operating condition prevents the dispatch of generator 22, whose participation would increase the marginal cost to its higher offer price. From a strategic viewpoint, the aggregator, whose objective is to minimise system balancing costs, bids its flexibility at a price aligned with the marginal cost of generator 21 rather than at the cost of generator 22, thereby mitigating price spikes in critical hours. It is important to note that, if the balancing requirement exceeded the maximum flexible power available, the aggregator would not be able to fully cover the imbalance and the entry of generator 22 would become unavoidable, restoring a higher marginal price.

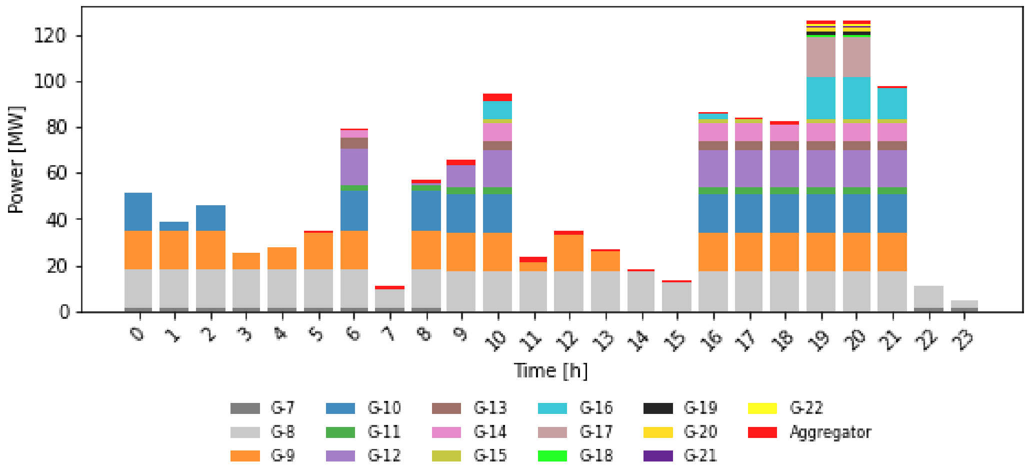

Figure 9. Hourly dispatch of thermal generators in the scenario with demand flexibility

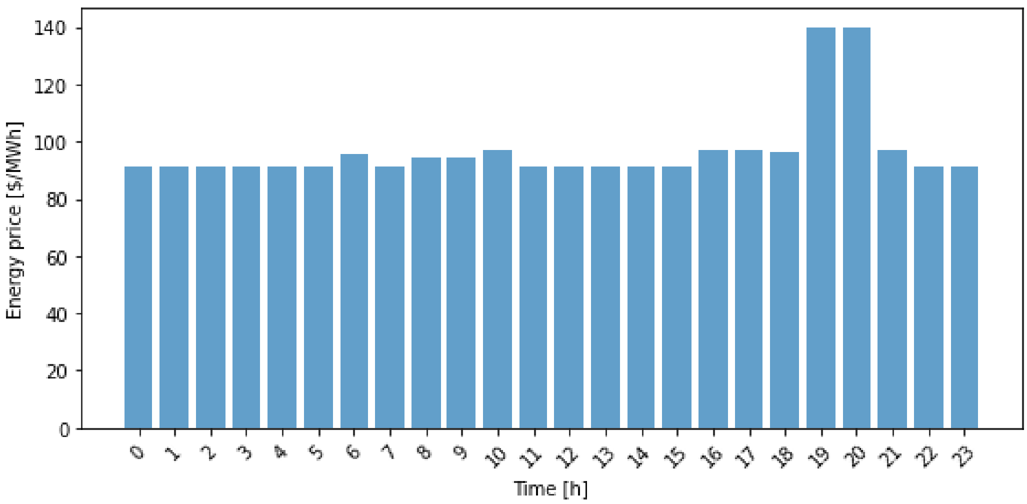

Figure 10. Energy prices in the scenario with demand flexibility.

From an economic perspective, and considering that the balancing cost is defined by the cost of the last unit that supplies energy to restore system balance, the aggregator obtains a daily revenue of USD 2475.15 from the provision of balancing services in the short-term market. However, its influence on price formation is mainly concentrated in peak hours, since in the remaining periods its flexible power is not large enough to displace the marginal generation units and reduce the energy price down to the level of the next-cheapest generator. Consequently, the aggregator behaves as a targeted flexibility resource, with a significant impact under stressed system conditions but a limited effect during low- and medium-demand intervals.

6.4. Impact of Demand Flexibility on Distribution Network Operation

The operation of the distribution network is assessed using technical indicators that enable a comparative evaluation of system performance under different loading conditions. These indicators are computed for two configurations: (i) without demand flexibility activation and (ii) with demand flexibility managed by the aggregator, in order to quantify its impact on network operation. Figure 11 depicts the topology of the local distribution network, including the distribution substations and the boundary points that interconnect it with the National Interconnected System. The different line colors are used solely as a visual identification criterion: each color corresponds to the feeders associated with a given substation, such that line segments sharing the same color belong to the same feeder group and facilitate the rapid identification of its area of influence within the network. Although the figure includes the 22 kV network to provide context for feeder interconnections, the analysis conducted in this study focuses on the subtransmission level (69 kV).

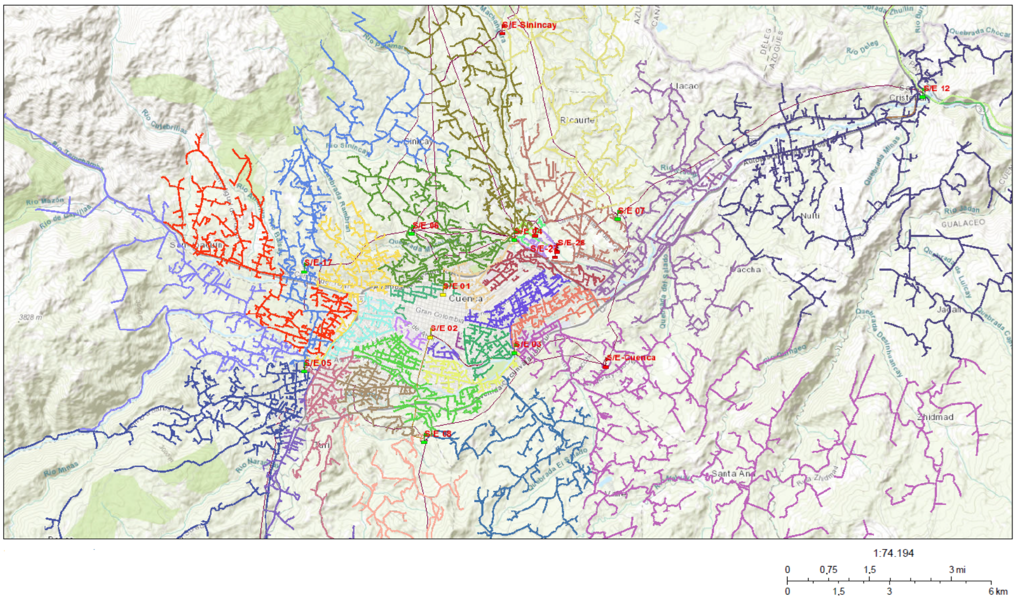

Figure 11. Geographical layout of the local electric utility distribution network. Source: [36]

The methodology relies on steady-state power flow simulations using daily demand profiles consistent with the solution of the aggregator model. This model provides the hourly demand profile of the large consumers in each scenario, from which the corresponding load vectors applied to the distribution network are constructed. On this basis, power flow studies are performed in DIgSILENT PowerFactory, automated through a Python subroutine. This integrated framework enables the calculation of bus voltages, line and transformer loading levels, and system losses for each case study and hourly interval, thereby facilitating a quantitative assessment of the impact of demand flexibility on the operation of the distribution company-owned and operated 69 kV subtransmission network.

6.4.1. Voltages Levels

The results in Table 2 indicate that the activation of demand flexibility has a clearly beneficial impact on the voltage profile of the most critical buses in the network. In the scenario without flexibility, bus HA 138 exhibits the worst performance, with a minimum voltage of 0.93 p.u. at 19:00, noticeably below the nominal level and associated with the evening peak demand. When flexibility is activated, its minimum voltage rises to 1.03 p.u. at the same hour, effectively eliminating the undervoltage condition. A similar improvement is observed at buses T142, Lentag–22 kV and T141, where the minimum voltage increases from 0.96 p.u. to 0.98–0.97 p.u., providing a larger operational margin with respect to the lower limits. At buses L. Cordero–6.3 kV and Centenario–6.3 kV the minimum voltage remains at 0.95 p.u., but still within the admissible range, while bus Méndez–138 does not experience significant changes. It is worth noting that the maximum voltages remain practically unchanged between scenarios and stay below 1.05 p.u.; therefore, the improvement in minimum voltage conditions is not accompanied by overvoltage problems, but rather reflects a more uniform utilisation of the network during peak hours due to the activation of flexible demand.

Table 2. Minimum and maximum bus voltages in scenarios with and without demand flexibility.

Bus	Without Demand Flexibility				With Demand Flexibility			
	$V_{\min}$ [p.u.]	$h(V_{\min})$	$V_{\max}$ [p.u.]	$h(V_{\max})$	$V_{\min}$ [p.u.]	$h(V_{\min})$	$V_{\max}$ [p.u.]	$h(V_{\max})$
L. Cordero–6.3 kV	0.95	11:00	0.96	5:00	0.95	11:00	0.96	5:00
Centenario–6.3 kV	0.95	12:00	0.96	6:00	0.95	12:00	0.96	6:00
HA 138	0.93	19:00	1.04	7:00	1.03	19:00	1.04	7:00
T142	0.96	19:00	0.96	6:00	0.98	19:00	0.96	6:00
Lentag–22 kV	0.96	19:00	0.96	6:00	0.97	19:00	0.96	6:00
T141	0.96	19:00	0.96	6:00	0.97	19:00	0.96	6:00
Méndez–138	1.03	19:00	1.04	8:00	1.03	19:00	1.04	8:00

6.4.2. Loading Lines

The results in Table 3 show that the activation of demand flexibility has a limited but measurable impact on the loading of the most critical subtransmission lines. In both scenarios, the maximum loading levels remain well below typical thermal limits, with the most heavily loaded circuit (Abanico–Macas) reaching about 49% of its capacity at 7:00, unaffected by the activation of flexibility. The remaining lines exhibit maximum loadings in the range of 30–46%, and the hours at which these maxima occur are essentially the same with and without flexibility, indicating that the global power flow pattern in the subtransmission network is preserved. However, small reductions can be observed in some circuits, such as P. Industrial(04)–L. Cordero(01) and Verdillo(06)–P. Industrial(04), where the maximum loading decreases by around 0.04–0.7 percentage points. These results suggest that, under the considered demand conditions, demand flexibility contributes marginally to relieving subtransmission loading. However, the network already operates with a comfortable margin with respect to line capacity, so congestion is not a binding constraint in either scenario.

Table 3. Maximum loading of subtransmission lines in scenarios with and without demand flexibility.

Line	Without Demand Flexibility		With Demand Flexibility	
	$L_{\max}$ [%]	$h(L_{\max})$	$L_{\max}$ [%]	$h(L_{\max})$
Abanico–Macas	49.38	7:00	49.38	7:00
Monay(03)–Turi(08)	45.47	19:00	45.47	19:00
Monay(03)–P. Centenario(02)s	42.66	12:00	42.66	12:00
P. Industrial(04)–L. Cordero(01)	39.09	11:00	39.05	11:00
Cuenca–Monay(03)	38.57	19:00	38.57	19:00
Verdillo(06)–SE 17	37.00	19:00	37.00	19:00
Cuenca 2–Verdillo (06)	36.99	19:00	36.99	19:00
Cuenca–Monay(03)–1	36.82	19:00	36.82	19:00
Verdillo(06)–P. Industrial(04)	35.14	11:00	34.41	11:00
Cuenca 2–Verdillo (06)	30.66	19:00	30.58	19:00

6.4.3. Loading Transformers

The results in Table 4 show that transformer loading is only moderately affected by the activation of demand flexibility, and that the most critical element remains overloaded in both scenarios. Transformer T121 operates slightly above its nominal capacity, with a maximum loading of 101.02% at 19:00 in the base case and 101.00% at the same hour when flexibility is activated, indicating that the available flexible demand is not sufficient to eliminate this structural overload. The remaining transformers operate with a more comfortable margin: TEEAz and TEEAz2 reach maximum loadings of approximately 90% and 82%, respectively, while T122 and T123 remain around 77–78%, with negligible differences between scenarios. The Abanico transformers exhibit maximum loadings close to 73% at 7:00, unaffected by flexibility. A slightly more noticeable effect is observed in transformer T061, whose maximum loading decreases from 63.58% at 11:00 to 62.27% at 14:00 with flexibility, reflecting both a reduction and a temporal shift of the peak. Overall, these results indicate that demand flexibility contributes marginally to relieving transformer loading and redistributing flows in time, but it does not fully resolve the overload at T121, suggesting that additional network reinforcements or reconfiguration measures are required to address this constraint.

Table 4. Maximum loading of transformers in scenarios with and without demand flexibility.

Transformer	Without Demand Flexibility		With Demand Flexibility	
	$L_{\max}$ [%]	$h(L_{\max})$	$L_{\max}$ [%]	$h(L_{\max})$
T121	101.02	19:00	101.00	19:00
TEEAz	90.11	19:00	90.09	19:00
TEEAz2	81.71	19:00	81.70	19:00
T122	77.95	19:00	77.94	19:00
T123	77.34	19:00	77.33	19:00
T Abanico	72.91	7:00	72.91	7:00
T Abanico b	72.48	7:00	72.48	7:00
T061	63.58	11:00	62.27	14:00
T131	58.37	19:00	58.37	19:00
T081	56.20	19:00	56.20	19:00

6.4.4. Losses

Based on the hourly loss results, the demand flexibility managed by the aggregator has a moderate but consistent effect on the system's technical losses. In the base scenario, without activating flexibility, the total energy lost over the day amounts to 89.46 MWh, whereas with flexibility this value decreases to 89.10 MWh, i.e., a reduction of 0.36 MWh (approximately 0.4%). The differences are concentrated mainly during high-load hours, when load reduction and interruption actions slightly flatten the power flow profile and consequently reduce the currents flowing through lines and transformers. However, since the network already operates with relatively low loading levels, the margin for improvement in terms of losses is limited. Therefore, the main contribution of flexibility is more clearly reflected in the mitigation of price spikes and the improvement of voltage profiles than in the reduction of energy losses.

7. Conclusions

The analysis shows that the proposed aggregator is able to coordinate the available flexibility from the 26 large consumers in an efficient manner, contributing to a partial reduction in system balancing costs and an improvement in some technical network indicators, particularly the voltage profile during peak hours. However, the results also reveal that the current portfolio of flexible resources is relatively limited: the available reducible and interruptible power is insufficient to remove structural overloads, such as those observed in transformer T121, or to produce substantial changes in subtransmission line loading. In this context, the aggregator behaves more like a local support resource than a dominant actor capable of deeply reshaping the network's operating state, highlighting the need to increase the amount of manageable flexibility if a more systemic impact is desired.

From a market design and policy perspective, the results suggest that, if the aggregator had access to larger blocks of flexible energy, it could influence not only real-time balancing costs but also day-ahead energy prices by displacing higher-cost marginal units. In the case study, this effect does not materialise precisely because of the limited volume of flexibility, which underscores the importance of incentivising the participation of additional large consumers and of establishing regulatory frameworks and price signals that promote active engagement in aggregation schemes. Furthermore, the inclusion of distributed energy resources (for example, photovoltaic generation and battery energy storage systems) would significantly expand the decision space of the aggregator and enable participation in ancillary service markets. However, this would require explicitly addressing the stochastic and intermittent nature of these resources, which is recognised as a more complex extension and is therefore proposed as future work. In this sense, the present model serves as an initial motivation and a clear proof of concept for the value that an aggregator can provide to both the power system and large consumers.

Finally, the results emphasise the importance of the geographical and electrical location, as well as the selection of participating users. It is not sufficient to have a given amount of flexibility in aggregate terms; it is necessary to identify "suitable" consumers at nodes where the network exhibits weaknesses (low voltages, high loading levels, or the need for reinforcement), so that the activation of flexibility yields a maximum technical benefit. Since demand-side response is significantly faster than the start-up or ramping of conventional generators, this characteristic offers a key operational advantage that should be exploited. However, the current aggregator model focuses exclusively on "upward" compensation, that is, on interruptible and reducible load, without yet considering load-shifting schemes. Implementing "downward" compensation would require differentiated demand contracts (e.g., DDL-type arrangements) that allow the transfer of consumption to other time periods with lower costs and reduced network stress. In addition, the optimal allocation of flexible resources among large consumers, considering both economic criteria and network technical constraints simultaneously, is identified as a relevant topic that is explicitly left for future research.

Author Contributions: Conceptualization, M.T.O.; methodology, M.T.O.; software, M.T.O. and F.H.C.; investigation, M.T.O., Y.B. and D.M.; validation, C.Á.B., D.M. and M.T.O.; formal analysis, M.T.O. and C.Á.B.; resources, J.B.C., M.T.O. and D.M.; data curation, M.T.O. and D.M.; writing original draft preparation, M.T.O. and F.H.C.; writing review, and editing, D.M., C.Á.B. and J.B.C.; supervision, C.Á.B.; project administration, M.T.O. and J.B.C. All authors read and agreed to the published version of this manuscript.

Funding: The PIC5P23-31 project funded this work: Production of plastic structures, urban furniture, ecological clothing, and footwear through the implementation of the Circular Economy.

Data Availability Statement: The data presented in this study are available upon request from the corresponding author due to data security and confidentiality requirements.

Conflicts of Interest: Author Freddy H. Chuqui is employed by the company Utiliy Electro Generadora del Austro. The remaining authors declare that the research was conducted in the absence of any commercial or financial relationships that could be construed as a potential conflict of interest.

https://doi.org/10.3390/en19010152

Abbreviations

The following abbreviations are used in this manuscript:

ADMM	Alternating Direction Method of Multipliers
ADMS	Advanced Distribution Management System
AMI	Advanced Metering Infrastructure
BESS	Battery Energy Storage System
BRP	Balance Responsible Party
CMSP	Congestion Management Service Provider
CSP	Curtailment Service Provider
DA	Day-Ahead
DF	Demand Flexibility
DER	Distributed Energy Resource
DMS	Distribution Management System
DR	Demand Response
DRIP	Demand Response in Industrial Production
DSO	Distribution System Operator
ECDIAC	Energy Consumption Dataset for Industrial Applications
EV	Electric Vehicle
FHMM	Factorial Hidden Markov Model
F1	F1-Score
FRP	Flexibility Requesting Party
IEC	International Electrotechnical Commission
LC	Large Consumer
LP	Linear Programming
MAPE	Mean Absolute Percentage Error
MDM	Meter Data Management
MILP	Mixed Integer Linear Programming
NILM	NonIntrusive Load Monitoring
NILMTK	Non Intrusive Load Monitoring Toolkit
P2P	Peer-to-Peer
PV	Photovoltaic
RF	Random Forest
RMSE	Root Mean Square Error
RT	Real Time
SAIDI	System Average Interruption Duration Index
SAIFI	System Average Interruption Frequency Index
TSO	Transmission System Operator
V2G	Vehicle-to-Grid

Nomenclature

The following nomenclature defines the sets, parameters, and variables used in the bi-level aggregator model:

Sets

T	Set of dispatch hours
G	Set of generators providing system balancing
GC	Set of LC participating in the DR program

Parameters

P_t^S	Day-ahead scheduled generation at hour t
P_t^B	Real-time balancing demand at hour t
Δt	Duration of each dispatch interval
$\overline{P_{t,i}^I}$	Maximum interruptible power of consumer i at hour t
$\overline{P_{t,i}^{\mathcal{R}}}$	Maximum reducible power of consumer i at hour t
$\overline{P_{t,i}^U}$	Maximum upward balancing power from generator i at hour t
$\overline{P_{t,i}^L}$	Maximum downward balancing power from generator i at hour t
$\overline{P_t^{A,\mathcal{B}_U}}$	Maximum upward balancing cleared by the aggregator at hour t
$\overline{P_t^{A,\mathcal{B}_L}}$	Maximum downward balancing cleared by the aggregator at hour t
$C_{t,i}^U$	Upward regulation cost of generator i at hour t
$C_{t,i}^L$	Downward regulation cost of generator i at hour t

Decision Variables

$P_t^{A,\mathcal{B}_U}$	Upward adjustment cleared by the aggregator in the short-term market at hour t
$P_t^{A,\mathcal{B}_L}$	Downward adjustment cleared by the aggregator in the short-term market at hour t
γ_t	Short-term market spot price at hour t
β_t	Aggregator's offer in the short-term market at hour t
$P_{t,i}^I$	Interruptible power of consumer i at hour t
$P_{t,i}^{\mathcal{R}}$	Reducible power of consumer i at hour t
$\alpha_{t,i}^I$	Binary variable indicating activation of the interruptible block of consumer i at hour t
$P_{t,i}^U$	Upward balancing power of generator i at hour t
$P_{t,i}^L$	Downward balancing power of generator i at hour t

References

1. Artificial Intelligence in Power Systems. *IEEE Power Energy Mag. (Edición En Español)* **2024**, *173*. Available online: https://resourcecenter.ieee-pes.org/publications/power-and-energy-magazine/pes_tp_mag_pe_v22_n6_sp (accessed on 14 December 2025).
2. Kumaran Nalini, B.; You, Z.; Zade, M.; Tzscheutschler, P.; Wagner, U. OpenTUMFlex: A flexibility quantification and pricing mechanism for prosumer participation in local flexibility markets. *Int. J. Electr. Power Energy Syst.* **2022**, *143*, 108382. [CrossRef]
3. Lei, X.; Zhong, J.; Chen, Y.; Shao, Z.; Jian, L. Grid integration of electric vehicles within electricity and carbon markets: A comprehensive overview. *eTransportation* **2025**, *25*, 100435. [CrossRef]
4. Tsaousoglou, G.; Giraldo, J.S.; Pinson, P.; Paterakis, N.G. Mechanism Design for Fair and Efficient DSO Flexibility Markets. *TechRxiv* 2020, *Preprint*. [CrossRef]
5. Jobran, H.; Manoochehri, H.; Fereidunian, A. Reinforced Restoration of Smart Distribution Systems Utilizing Transactive Flexibility of Prosumers. In Proceedings of the 12th Smart Grid Conference (SGC), Tehran, Iran, 13–15 December 2022. Available online: https://www.researchgate.net/publication/366856970_Reinforced_Restoration_of_Smart_Distribution_Systems_Utilizing_Transactive_Flexibility_of_Prosumers (accessed on 14 December 2025).
6. 2025 PES Grid Edge Technologies Conference & Exposition: Official Show Issue and Program. *IEEE Power Energy Mag. (Edición En Español)* **2025**, *142*. Available online: https://resourcecenter.ieee-pes.org/publications/power-and-energy-magazine/pes_tp_mag_pe_v23_n1_sp (accessed on 14 December 2025).
7. Burgos, A.; Correa, C.; Finot, J.; Granda, C.; Hill, B.; Maquieira, C. *Navigating the Energy Transition in Latin America and the Caribbean: Volatility and Price-Signaling in Short-Term Electricity Markets*; Technical Note IDB-TN-2847; Inter-American Development Bank (IDB): Washington, DC, USA, 2024.
8. Schaffitzel, F.; Jakob, M.; Soria, R.; Vogt-Schilb, A.; Ward, H. *¿Pueden las transferencias del gobierno hacer que la reforma de los subsidios energéticos sea socialmente aceptable? Un estudio de caso sobre Ecuador*; Documento de Trabajo IDB-WP-1026; Banco Interamericano de Desarrollo (BID): Washington, DC, USA, 2019.
9. Offshore Wind Energy. *IEEE Power Energy Mag. (Edición En Español)* **2024**, *149*. Available online: https://resourcecenter.ieee-pes.org/publications/power-and-energy-magazine/pes_tp_mag_pe_v22_n5_sp (accessed on 14 December 2025).
10. Equity and Justice in Power Systems. *IEEE Power Energy Mag. (Edición En Español)* **2024**, *142*. Available online: https://resourcecenter.ieee.org/publicaciones/revista-potencia-y-energia/pes_tp_mag_pe_v22_n4_sp (accessed on 14 December 2025).

11. Rodríguez-García, J.; Ribó-Pérez, D.; Álvarez Bel, C.; Peñalvo-López, E. Maximizing the Profit for Industrial Customers of Providing Operation Services in Electric Power Systems via a Parallel Particle Swarm Optimization Algorithm. *IEEE Access* **2020**, *8*, 24721–24733. [CrossRef]
12. Toledo-Orozco, M.; Celi, C.; Guartan, F.; Peralta, A.; Álvarez Bel, C.; Morales, D. Methodology for the disaggregation and forecast of demand flexibility in large consumers with the application of non-intrusive load monitoring techniques. *Energy AI* **2023**, *13*, 100240. [CrossRef]
13. Rodríguez, F.; Maqueda, E.; Fernández, M.; Pimenta, P.; Inês Marques, M. A novel methodology for day-ahead buildings energy demand forecasting to provide flexibility services in energy markets. *Int. J. Electr. Power Energy Syst.* **2024**, *161*, 110207. [CrossRef]
14. Savelli, I.; Bokkisam, H.R.; Cuffe, P.; Morstyn, T. On-demand energy flexibility market via smart contracts to help reduce balancing costs in Great Britain. *Energy Econ.* **2023**, *126*, 106931. [CrossRef]
15. Cabot, C.; Villavicencio, M. The demand-side flexibility in liberalised power market: A review of current market design and objectives. *Renew. Sustain. Energy Rev.* **2024**, *201*, 114643. [CrossRef]
16. Moradi, M.; Farzaneh, H. Hybrid local energy markets in Japan: Assessing the impact of regional renewable energy integration, demand flexibility, and consumer behavior. *Energy Convers. Manag. X* **2025**, *27*, 101075. [CrossRef]
17. Nasab, M.A.; Alizadeh, M.; Nasimov, R.; Zand, M.; Nasab, M.A.; Padmanaban, S. Planning with the electricity market One day ahead for a smart home connected to the RES by the MILP method. *Renew. Energy Focus* **2024**, *50*, 100606. [CrossRef]
18. Toledo-Orozco, M.; Morales Jadán, D.; Arévalo Lozado, S.; Álvarez Bel, C. Methodological Planning to Determine the Technological Expansion of Smart Metering Systems for Utilities. *Energies* **2024**, *17*, 4603. [CrossRef]
19. Özge Okur.; Heijnen, P.; Lukszo, Z. Aggregator's business models in residential and service sectors: A review of operational and financial aspects. *Renew. Sustain. Energy Rev.* **2021**, *139*, 110702. [CrossRef]
20. Hincapié Correa, J.A. Evaluación de un Modelo de Agregadores de Demanda en el Sistema Eléctrico Colombiano. Master's Thesis, Universidad Nacional de Colombia, Medellín, Colombia, 2022.
21. Backe, S.; Delgado, B.M.; Askeland, M.; Walnum, H.T.; Sørensen, Å.L.; Sartori, I. Impact of activating energy demand flexibility in the building stock: A case study of Norway as a highly electrified country in the European power market. *Energy* **2025**, *318*, 134688. [CrossRef]
22. Askeland, M.; Bjarghov, S.; Rana, R.; Morch, A.; Taxt, H. Smart flexibility in energy communities: Scenario-based analysis of distribution grid implications and economic impacts. *Smart Energy* **2025**, *18*, 100184. [CrossRef]
23. Syla, A.; Parra, D.; Patel, M.K. Assessing flexibility from electric vehicles using an open-source energy system model: Trade-offs between smart charging, vehicle-to-grid and an extensive charging infrastructure. *Energy* **2025**, *326*, 136236. [CrossRef]
24. Messias, R.; Carvalho, P.M.; Sousa, J. Welfare-maximizing market procurement of flexibility services for distribution network planning. *Util. Policy* **2026**, *98*, 102086. [CrossRef]
25. Shepherd, M.M.; Mohagheghi, S. Demand Flexibility: A Review of Quantification Methods, Models, and Required Data. *Appl. Sci.* **2024**, *14*, 1276. [CrossRef]
26. Makonin, S.; Popowich, F.; Bartram, L.; Gill, B.; Bajic, I.V. AMPds: A public dataset for load disaggregation and eco-feedback research. In Proceedings of the IEEE Electrical Power and Energy Conference, Halifax, NS, Canada, 21–23 August 2013 ; pp. 1–6. [CrossRef]
27. Zhao, Y.; Peng, K.; Xu, B.; Li, H.; Liu, Y.; Zhang, X. Bilevel optimal dispatch strategy for a multi-energy system of industrial parks by considering integrated demand response. *Energies* **2018**, *11*, 1942. [CrossRef]
28. Rodríguez-García, J.; Álvarez Bel, C.; Carbonell-Carretero, J.F.; Escrivá-Escrivá, G.; Calpe-Esteve, C. Design and validation of a methodology for standardizing prequalification of industrial demand response resources. *Electr. Power Syst. Res.* **2018**, *164*, 220–229. [CrossRef]
29. Lu, X.; Li, K.; Xu, H.; Wang, F.; Zhou, Z.; Zhang, Y. Fundamentals and business model for resource aggregator of demand response in electricity markets. *Energy* **2020**, *204*, 117885. [CrossRef]
30. He, Y.; Vahidinasab, V.; Pinson, P. Aggregator's role and business models in smart grid demand response markets: Review and future trends. *Appl. Energy* **2020**, *261*, 114335. [CrossRef]
31. *IEC 61968-1*; Application Integration at Electric Utilities—System Interfaces for Distribution Management—Part 1: Interface Architecture and General Recommendations. International Electrotechnical Commission (IEC): Geneva, Switzerland, 2020.
32. Taha, H.A. *Operations Research: An Introduction*, 10th ed.; Pearson: Boston, MA, USA, 2017.
33. Hillier, F.S.; Lieberman, G.J. *Introduction to Operations Research*, 10th ed.; McGraw-Hill Education: New York, NY, USA, 2020.
34. Winston, W.L. *Operations Research: Applications and Algorithms*, 4th ed.; Duxbury Press: Belmont, CA, USA, 2004.

35. Fortuny-Amat, I.; McCarl, B.A. A representation and economic interpretation of a two-level programming problem. *J. Oper. Res. Soc.* **1981**, *32*, 783–792. [CrossRef]
36. Naula, D.J.C.; Cajamarca, F.H.C. Modelo de optimización multietapa para la planificación de la expansión de subestaciones del sistema de subtransmisión de la Empresa Eléctrica Regional Centro Sur C.A. Master's Thesis, Universidad de Cuenca, Cuenca, Ecuador, 2021.